

# Architecture Design, Frequency Planning, and Performance Analysis for a Microcell/Macrocell Overlaying System

Li-Chun Wang, *Member, IEEE*, Gordon L. Stüber, *Senior Member, IEEE*, and Chin-Tau Lea, *Senior Member, IEEE*

**Abstract**—An innovative hierarchical microcell/macrocell architecture is presented. By applying the concept of *cluster planning*, the proposed sectoring arrangement can provide good shielding between microcells and macrocells. As a result, underlaid microcells can reuse the same frequencies as overlaying macrocells without decreasing the macrocell system capacity. With the proposed method, microcells not only can be gradually deployed, but they can be extensively installed to provide complete coverage and increase capacity throughout the service area. With these flexibilities, the proposed method allows existing macrocellular systems to evolve smoothly into a hierarchical microcell/macrocell architecture.

**Index Terms**—Cluster planning, hierarchical cellular architecture, macrocell/microcell overlaying system.

## I. INTRODUCTION

HIERARCHICAL microcell/macrocell architectures have been proposed for future personal communications systems [1]. These architectures provide capacity relief to a macrocell system and offer many advantages over a pure microcell system. Unlike the pure microcell system, which requires extensive microcell base-station (BS) deployment throughout the whole service area, a hierarchical architecture allows gradual deployment of microcells as user demand increases. The hierarchical architecture also protects investment cost in the existing macrocellular system, while a pure microcell system requires replacement of the macrocell BS's. Furthermore, the fast handoff requirement in a pure microcell system can be relieved in the overlaying architecture by temporarily connecting the call to a macrocell BS [2].

The method of sharing the radio spectrum is the key issue for hierarchical microcell/macrocell systems. Different kinds of frequency sharing schemes have been proposed in the literature [3]–[5]. Orthogonal sharing partitions the frequency channels into two disjoint sets: one for macrocells and one for microcells [3]. Channel borrowing requires that the underlaid microcells utilize the free channels of adjacent macrocells [4]. A overlaying scheme that combines dynamic channel allocation (DCA) and power control is proposed in [5]. Each of the above schemes has some problems. Orthogonal sharing

[3] decreases the macrocell system capacity if the available spectrum has already been assigned to macrocells. Channel borrowing [4] can only relieve hot-spot traffic, but it is ineffective if the neighboring cells also have heavy traffic. The scheme in [5] requires power control (both uplink and downlink) and DCA, both of which will increase implementation cost.

This paper introduces an innovative hierarchical microcell/macrocell architecture to circumvent the above trade-offs. Under the proposed architecture, microcells can reuse the macrocell frequencies and will not decrease the macrocell system capacity. Furthermore, unlike the channel-borrowing scheme, which is effective only when the neighboring cells have free channels, the proposed architecture allows the microcells to be deployed throughout the whole service area regardless of the traffic loading of the neighboring macrocells. Compared to the system in [5], our architecture neither requires DCA nor downlink power control.

The remainder of this paper is organized as follows. Section II describes the system architecture. Section III offers a frequency planning algorithm to identify the low-interference macrocell frequencies that can be used in the microcells. Section IV describes the propagation model and system assumptions. The cochannel interference performance of the overlaying macrocells and underlaid microcells are discussed in Sections V and VI. The adjacent channel interference is discussed in Section VII. We conclude our discussion in Section VIII.

## II. SYSTEM ARCHITECTURE

Fig. 1 shows a traditional three-sector  $N = 7$  cellular system, where each cell consists of three sectors and  $N$  is the number of cells per cluster. In this system, the total channels are partitioned into 21 sets. The channel sets are assigned to the sectors so as to satisfy the frequency reuse constraint, e.g., channel set  $4_\beta$  in Fig. 1. The widely distributed cochannel interference makes it difficult to reuse the channel sets outside of their designated sectors. In the following, we introduce a *cluster planning* procedure to change the conventional sectoring scheme into a new structure.

### A. Cluster Planning Procedure

- 1) Assign the same channels to each cell site as in the traditional three-sector  $N = 7$  cellular system (Fig. 1),

Manuscript received August 11, 1995; revised May 21, 1996. This work was supported by Nortel and the National Science Foundation under Contract NCR-9523969.

L.-C. Wang is with AT&T Labs—Research, Red Bank, NJ 07701 USA. G. L. Stüber and C.-T. Lea are with the School of Electrical and Computer Engineering, Georgia Institute of Technology, Atlanta, GA 30332 USA. Publisher Item Identifier S 0018-9545(97)05113-X.

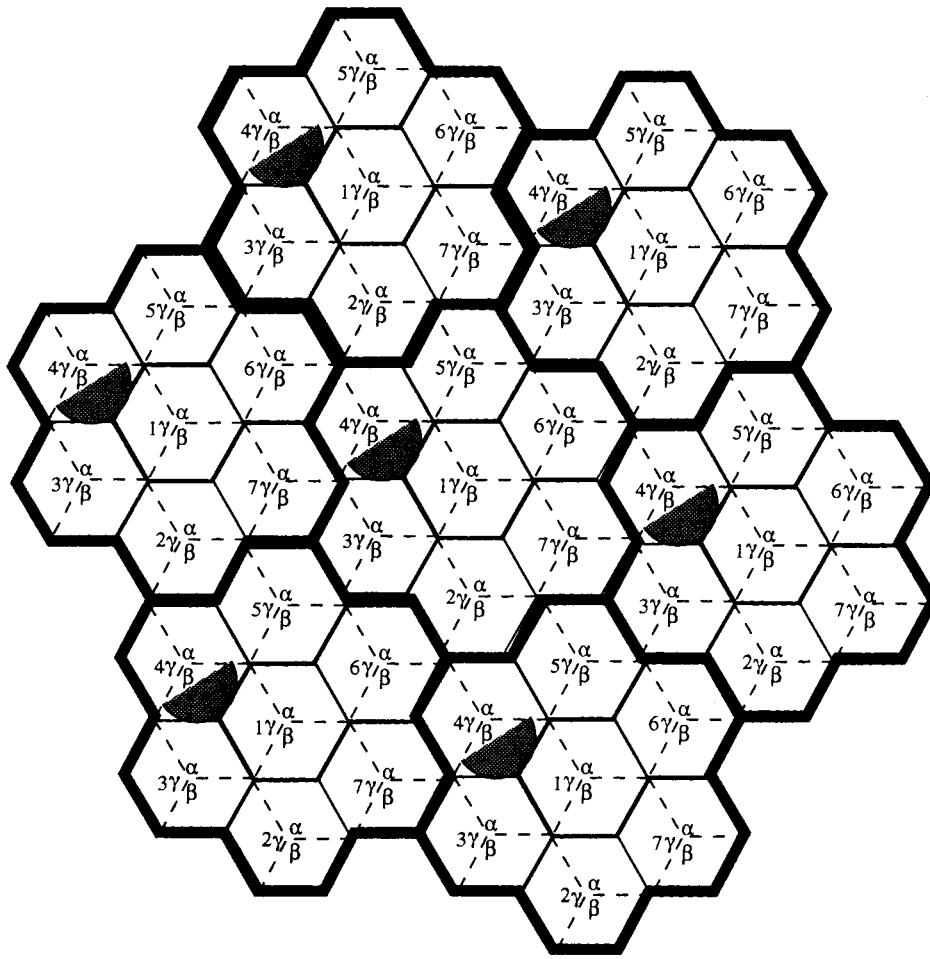


Fig. 1. Traditional three-sector  $N = 7$  cellular system.

where seven cells form a cluster and share the entire spectrum.

- 2) Divide macrocell clusters into three adjacent groups (Fig. 2).
- 3) Let the first group be the reference group.
- 4) Rotate the channel sets of the sectors in the second group  $120^\circ$  clockwise with respect to the first group.
- 5) Rotate the channel sets of the sectors in the third group  $120^\circ$  counterclockwise with respect to the first group.

Based on the above procedure, the sector rotations create low-interference regions outside the areas of the designated macrocell sectors for each channel set. These low-interference regions are called *microareas*. Fig. 3 shows the result of rotating the sectors. We see that zones A ~ F have a very low interference for channel set  $4_\beta$  since they are located in the back-lobe areas of the macrocell sectors using channel set  $4_\beta$ . Thus, microcells in these areas can use channel set  $4_\beta$ .

### III. UNDERLAID MICROCELL PLANNING ALGORITHM

As shown in Section II, microcells in the proposed architecture that are located in microareas can reuse certain macrocell channel sets. To have a greater flexibility in selecting the microcell BS locations, it is important that we identify all possible microareas and the available channels sets. In

our system, macrocells use frequencies on the front-lobe area of their directional antennas, while microcells reuse the same frequencies on the back-lobe area. In the conventional three-sector  $N = 7$  cellular system (Fig. 1), the back-lobe area of each channel set will still encounter some first-ring interferers. To protect the back-lobe areas from the first-tier interferers, we rotate the sectors through the cluster planning procedure described in Section II. Cluster planning creates low-interference microareas, as shown in Fig. 3, which lie in the back-lobe areas of the first-tier interferers. For ease of indexing, a microarea denotes a region of three adjacent macrocell sectors, each of which belongs to a different BS. Fig. 4 shows an example of a microarea. Each microarea has an *interference neighborhood*, defined as the 18 neighboring macrocell sectors that surround the microarea.

Let  $\Psi_i^j$  represent the channel set in the sector  $i$  ( $i = \alpha, \beta$ , and  $\gamma$ ) of cell site  $\Psi$  ( $\Psi = 1 \sim 7$ ); associate the superscript  $j$  in  $\Psi_i^j$  ( $j = 1 \sim 3$ ) with three types of cluster rotations:  $-120^\circ$ ,  $0^\circ$ , and  $120^\circ$ . Then, the following interesting observation can be made.

#### A. Observation

Consider a microarea and its interference neighborhood. A microarea can be located in the back-lobe area of the sectors

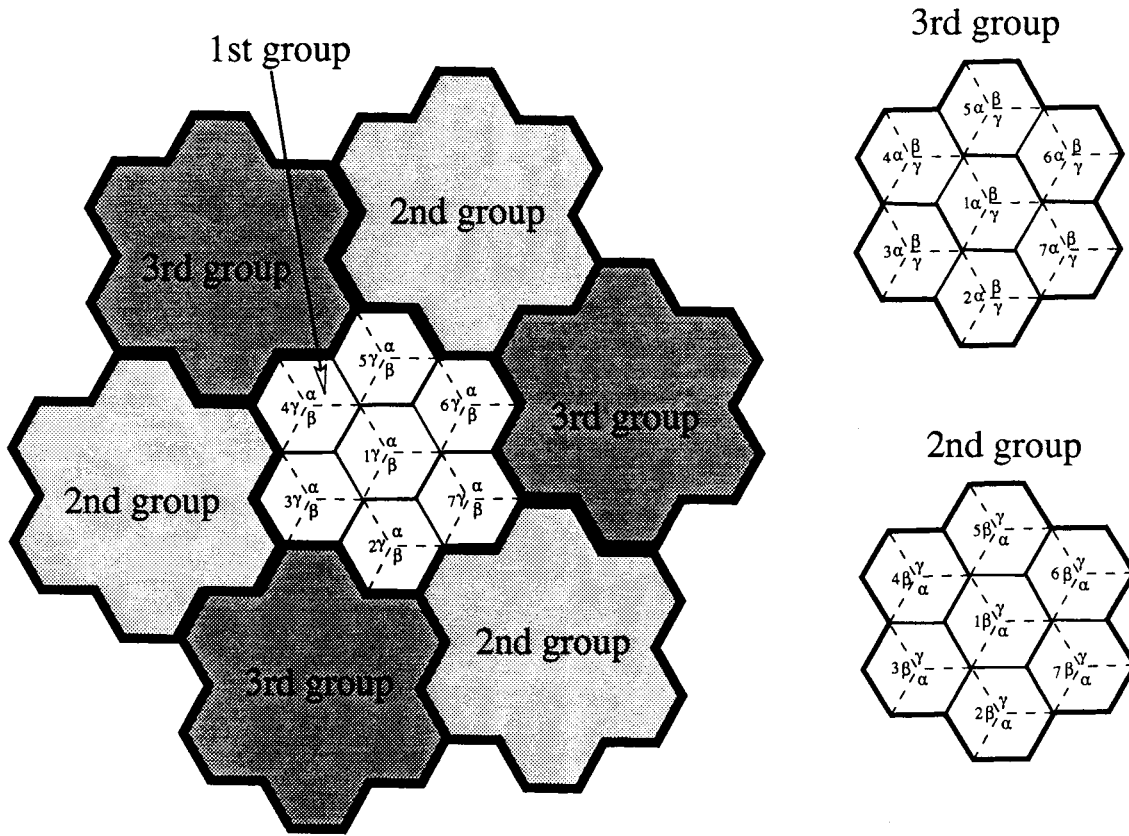


Fig. 2. Cluster planning for the proposed system.

using channel sets  $\Psi_\beta^j$  and  $\Psi_\gamma^j$  ( $j = 1 \sim 3$ ) if and only if it is surrounded by the main-lobe of three cochannel macrocell sectors using channel set  $\Psi_\alpha^j$ ; ( $j = 1 \sim 3$ ).

Based on the above observation, the following algorithm has been developed to determine the macrocell channel sets that can be reused in a microarea.

### B. Macrocell Channel-Selection Algorithm

- 1) Objective: identify low-interference macrocell channels that can be reused in the underlaid microcells.
- 2) For any microarea and its interference neighborhood  $M$ , let

$$\Theta = \{\Psi_i^j \in M\}$$

denote the union of channel sets  $\Psi_i^j$  that are used in  $M$ .

- 3) From  $\Theta$ , a  $3 \times 3$  indicator matrix  $\mathbf{B}_\Psi = [b_{ij}]$  is constructed for cell cites  $\Psi = 1 \sim 7$ , where

$$b_{ij} = \begin{cases} 1, & \text{if the channel set } \Psi_i^j \in M \\ 0, & \text{otherwise.} \end{cases}$$

- 4) If a certain indicator matrix  $\mathbf{B}_\Psi$  has a row of ones and two rows of zeros, then the zero rows of  $\mathbf{B}_\Psi$  correspond to the macrocell channel sets available for the microarea.

1) *Example:* We illustrate the above algorithm by the following example. According to Figs. 3 and 4, the interference neighborhood of microarea  $A$  is

$$\{\Theta = \{1_\alpha^2, 1_\beta^2, 1_\gamma^2, 2_\alpha^2, 2_\beta^2, 2_\gamma^2, 3_\alpha^2, 3_\beta^2, 3_\gamma^2, 4_\alpha^1, 4_\beta^1, 4_\gamma^1, 5_\alpha^1, 5_\beta^1, 5_\gamma^1, 6_\alpha^2, 6_\beta^2, 6_\gamma^2, 7_\alpha^2, 7_\beta^2, 7_\gamma^2\},$$

The indicator matrices are

$$\begin{aligned} \mathbf{B}_1 &= \begin{pmatrix} 0 & 1 & 0 \\ 0 & 1 & 0 \\ 0 & 1 & 0 \end{pmatrix} & \mathbf{B}_2 &= \begin{pmatrix} 0 & 1 & 0 \\ 0 & 1 & 0 \\ 0 & 1 & 0 \end{pmatrix} \\ \mathbf{B}_3 &= \begin{pmatrix} 0 & 1 & 1 \\ 0 & 0 & 0 \\ 0 & 1 & 0 \end{pmatrix} & \mathbf{B}_4 &= \begin{pmatrix} 1 & 1 & 1 \\ 0 & 0 & 0 \\ 0 & 0 & 0 \end{pmatrix} \\ \mathbf{B}_5 &= \begin{pmatrix} 1 & 1 & 0 \\ 0 & 0 & 0 \\ 1 & 0 & 0 \end{pmatrix} & \mathbf{B}_6 &= \begin{pmatrix} 0 & 1 & 0 \\ 0 & 1 & 1 \\ 0 & 0 & 0 \end{pmatrix} \\ \mathbf{B}_7 &= \begin{pmatrix} 0 & 1 & 0 \\ 0 & 1 & 0 \\ 0 & 1 & 0 \end{pmatrix}. \end{aligned}$$

Examination of the indicator matrices  $\mathbf{B}_\Psi$  ( $\Psi = 1 \sim 7$ ) reveals that  $\mathbf{B}_4$  is the only matrix having a row of ones and two rows of zeros; the second row and the third rows of  $\mathbf{B}_4$  are the zero rows. According to the above algorithm,  $4_\beta$  and  $4_\gamma$  are the low-interference macrocell channel sets available for use in microarea  $A$ . To see if microcells can be established in any location, we have examined a system with more microareas in Fig. 5. Through the above channel-selection algorithm, Table I shows that each microarea in the service area can reuse two macrocell channel sets. Recall that a microarea represents an area of three macrocell sectors, each of which belongs to three different cell sites. Thus, a macrocell area can has five channel sets—three for macrocells and two for microcells. In a macrocell area, each of three macrocell

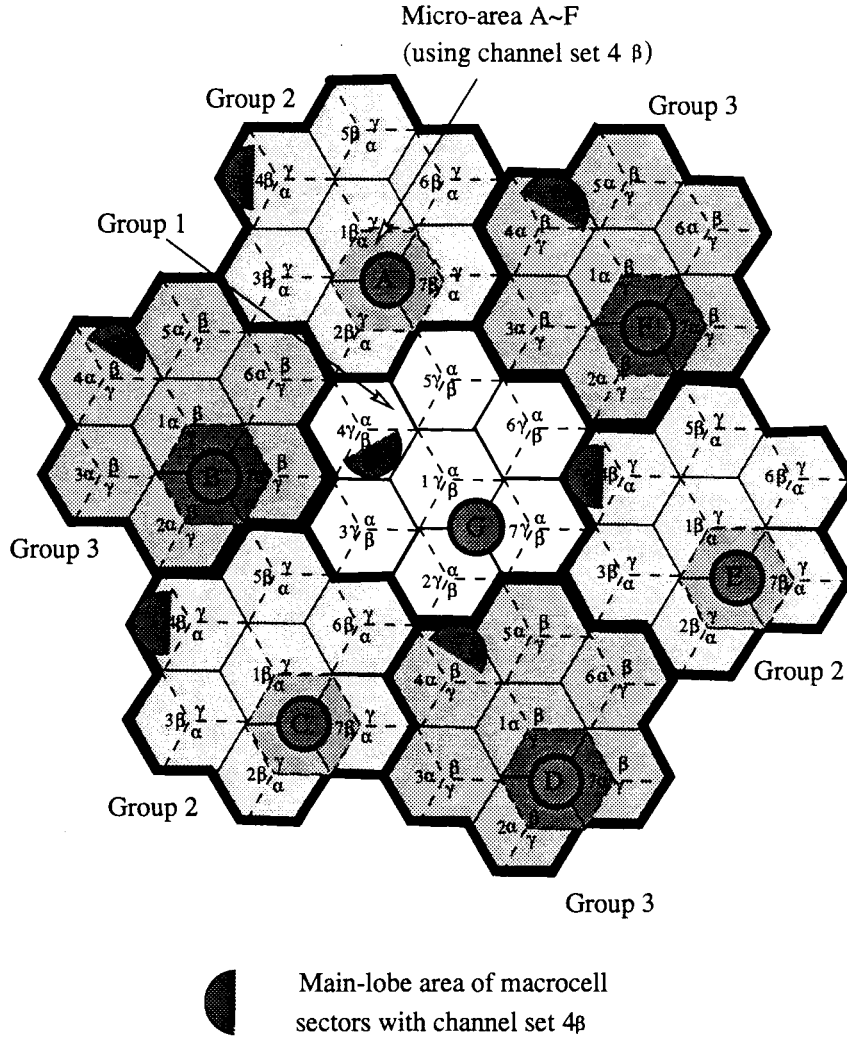


Fig. 3. Example of the proposed microcell/macrocell overlaying system. Microcells in microarea A ~ F can reuse the low-interfering macrocell channel set  $4\beta$ .

sectors reuses its channel sets only once, while a microarea can reuse its two macrocell channel sets many times, say  $C_\mu$  times, with a suitable cochannel reuse distance. Thus, it is implied that a macrocell area can use  $3 + 2 \times C_\mu$  channel sets simultaneously. Compared with three channel sets in the conventional three-sector macrocell, the system capacity of the proposed architecture increases by a factor of  $1 + 2 \times C_\mu/3$  times.

#### IV. PROPAGATION MODEL AND SYSTEM ASSUMPTIONS

##### A. Propagation Model

Our analysis considers the simple path-loss model [7]

$$p_r = \frac{p_t(h_b h_m)^2}{d^4} \quad (1)$$

where  $p_r$  and  $p_t$  are the received and transmitted powers,  $h_b$  and  $h_m$  are the antenna heights of the BS and the mobile station (MS), respectively, and  $d$  is the distance between the transmitter and receiver. Note that we incorporate the antenna gains in the transmitted power. Although (1) is derived from

a macrocell environment, it is still applicable to characterize the path loss outside the microcells [3].

##### B. Assumptions

1) *Interference*: In the hierarchical architecture, we consider four types of cochannel interference. In addition to the usual macrocell-to-macrocell and microcell-to-microcell cochannel interference, we must also consider macrocell-to-microcell and microcell-to-macrocell cochannel interference. Adjacent channel interference is also discussed in Section VII.

2) *Antenna*: The macrocell BS's are assumed to use  $120^\circ$  directional antennas, while microcell BS's use omnidirectional antennas. The MS also uses omnidirectional antennas.

3) *Uplink Power Control*: In this paper, we adopt the power control scheme used in IS-54 and AMPS systems [6]. The transmitted power of Class-IV IS-54 portable handsets is adjusted in six levels from  $-22$  to  $-2$  dBW in steps of 4 dB. Downlink power control is not required in the proposed architecture. Before proceeding, we first clarify our notation. When  $M$  and  $\mu$  are used, they represent macrocells and microcells, respectively; when  $m$  and  $b$  are used, they denote the MS and BS, respectively; when  $d$  and  $u$  are used, they

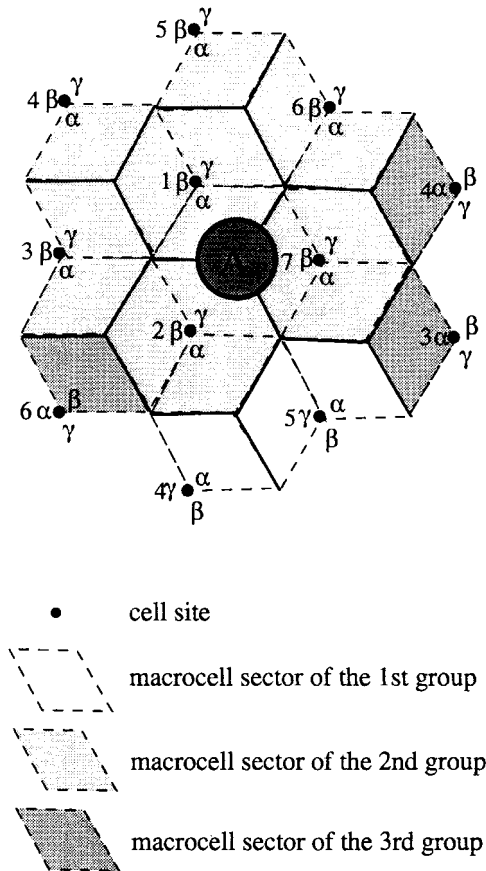


Fig. 4. Interfering neighborhood for microarea A in Fig. 3.

indicate the downlink (BS-to-MS) and uplink (MS-to-BS), respectively.

## V. MACROCELL PERFORMANCE

As shown in Section II, the new cluster planning technique with sector rotation can create some low-interference regions so that microcells can reuse macrocell frequencies. Nevertheless, some macrocells will experience higher interference after rotating the sectors. To evaluate the influence of the sector rotations on the macrocell performance, we simulate both the conventional macrocellular system (Fig. 1) and the proposed hierarchical cellular system (Fig. 3) without the underlaid microcells. Fig. 6 shows the simulation results of the uplink signal-to-interference (S/I) performance for both systems, assuming that the MS's are uniformly distributed in each sector and they transmit with the maximum power. We consider the uplink case because performance is usually better in the downlink than in the uplink [3]. With respect to 90% coverage probability, one can observe that the sector rotation technique creates low-interference regions at the cost of about 3.1, 3.3, and 3.5 dB S/I degradation for path-loss exponent  $\beta = 3.6, 3.8,$  and  $4.0$ . It is noteworthy that even after sector rotations, the macrocell can maintain S/I higher than 20 dB in 90% of the coverage area. In the following, we further include the underlaid microcells to analyze the performance of the proposed hierarchical cellular system. For ease of analysis, we hereafter adopt the worst case scenario, i.e., when an MS is on the cell boundary.

### A. Downlink Cochannel Interference Analysis

By applying (1), we express the signal-to-interference ratio (S/I) received by the MS at the macrocell boundary as

$$\frac{S_M^d}{I_M^d + J_{\mu M}^d} = \frac{p_{t,b}^M \frac{(h_b^M h_m)^2}{R_M^4}}{\sum_{i=1}^{N_M} \frac{p_{t,b}^M (h_b^M h_m)^2}{D_i^4} + \sum_{j=1}^{Z_\mu} \sum_{k=1}^{C_\mu} \frac{p_{t,b}^\mu (h_b^\mu h_m)^2}{d_{j,k}^4}} \quad (2)$$

where

$S_M^d$	MS received power from the desired macrocell BS;
$I_M^d$	downlink macrocell-to-macrocell interference;
$J_{\mu M}^d$	downlink microcell-to-macrocell interference;
$p_{t,b}^M$	macrocell BS transmitted power;
$p_{t,b}^\mu$	microcell BS transmitted power;
$N_M$	number of macrocell interferers;
$Z_\mu$	number of interfering microareas;
$C_\mu$	number of microcell clusters in a microarea;
$D_i$	MS distance to the $i$ th interfering macrocell BS;
$d_{j,k}$	MS distance to the $k$ th interfering microcell BS in the $j$ th microarea;
$h_b^M$	macrocell BS antenna height;
$h_b^\mu$	microcell BS antenna height;
$h_m$	MS antenna height;
$R_M$	macrocell radius.

Referring to Fig. 5 and Table I, we examine the downlink interference when a macrocell MS using channel set  $1_\beta$  is located at the macrocell boundary near microarea 56. One can find that the macrocell-to-macrocell downlink interference  $I_M^d$  mainly comes from the two first-tier macrocell BS's near microareas 77 and 68 with distances  $[D_1, D_2] = [4, 3.61]R_M$ . However, we also consider the three second-tier interfering BS's near microareas 11, 17, and 62 at distances  $[D_3, D_4, D_5] = [8.89, 8.89, 8.72]R_M$ . For the microcell-to-macrocell downlink interference  $J_{\mu M}^d$ , one can find six interfering microareas 35, 48, 54, 80, 86, and 99 in the first tier with distances  $[\bar{d}_1, \bar{d}_2, \bar{d}_3, \bar{d}_4, \bar{d}_5, \bar{d}_6] = [3, 4.58, 3.46, 6, 5.2, 6.25]R_M$ . The second-tier interfering microareas 3, 29, 41, and 92 have distances  $[\bar{d}_7, \bar{d}_8, \bar{d}_9, \bar{d}_{10}] = [7.55, 9, 7.94, 12]R_M$ . We assume that each microarea has  $C_\mu$  microcell reuse clusters, with each cluster having  $K_\mu$  microcells. Through the channel-selection algorithm in Section III, each microarea is assigned two macrocell channel sets. We further partition these two sets of channels into  $K_\mu$  groups and then assign each group to the  $K_\mu$  microcells in each cluster. In this manner, a macrocell channel set is used  $C_\mu$  times in a microarea. For ease of analysis, we assume that the distance  $\bar{d}_j$  approximates  $d_{j,k}$ , where  $\bar{d}_j$  is the distance from a macrocell MS to the center of the  $j$ th interfering microarea and  $d_{j,k}$  is defined in (2). In our example, the microcell BS antenna height is one third of macrocell BS antenna height, i.e.,  $h_b^\mu/h_b^M = 1/3$ . With the above assumptions in (2)

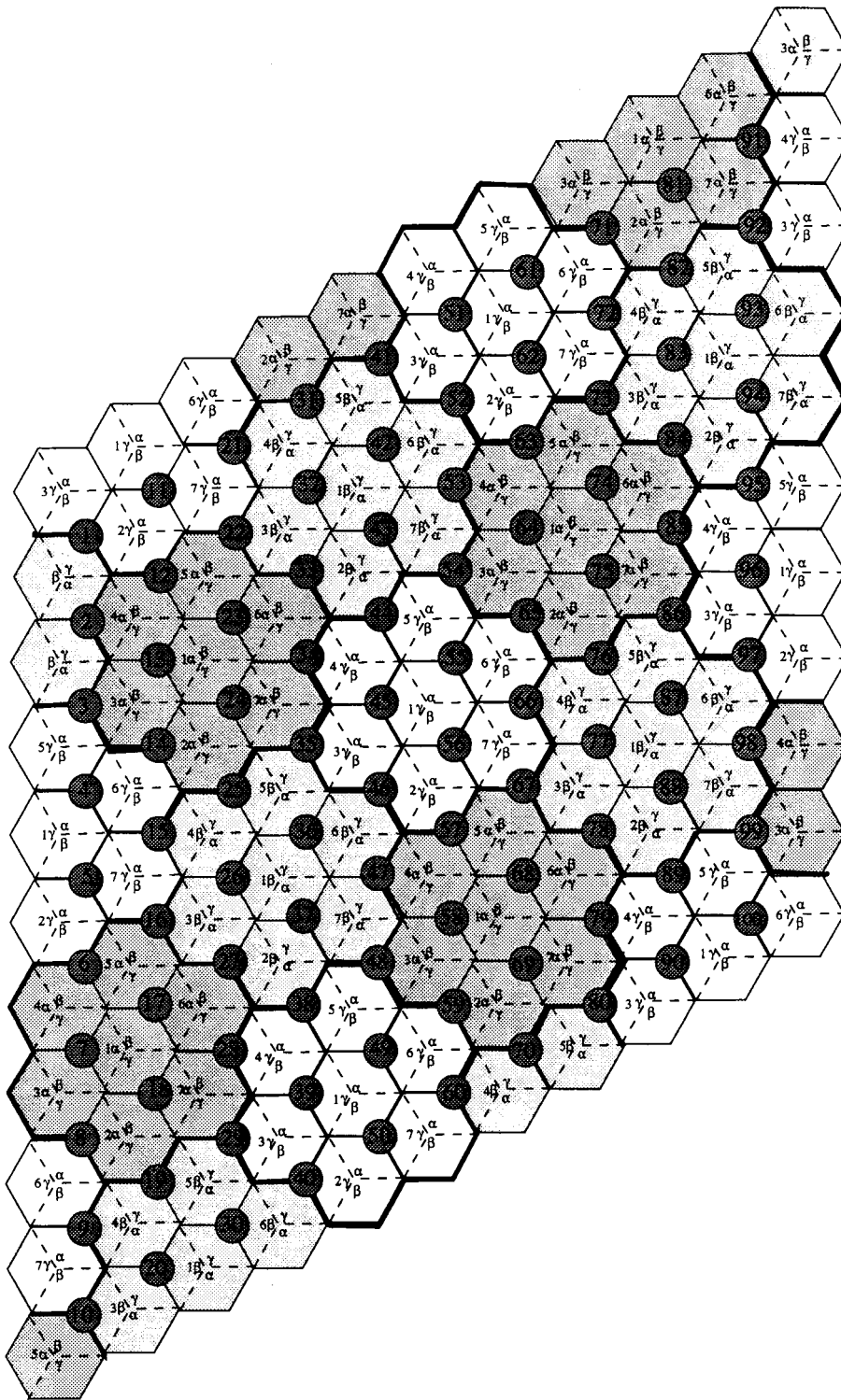


Fig. 5. Frequency planning for the proposed system with 100 microareas. Table I lists the available channel sets for the above 100 microareas.

$$\frac{S_M^d}{I_M^d + J_{\mu M}^d} = \frac{1}{1.02875 \times 10^{-2} + C_\mu \left( \frac{P_{t,b}^\mu}{P_{t,b}^M} \right) \times 2.79449 \times 10^{-3}}$$

We show the downlink S/I performance in terms of  $C_\mu$  and  $P_{t,b}^\mu/P_{t,b}^M$  in Fig. 7 with consideration of only first-tier interfering BS's; in Table II, with considerations of both first- and second-tier interfering BS's. Observe that  $S/I \geq 18$  dB for  $C_\mu = 6$  and  $P_{t,b}^\mu/P_{t,b}^M \leq 0.3$ . In other words, the channel set  $4_\beta$  can be reused six times in the microarea while still keeping the macrocell downlink S/I greater than 18 dB. Furthermore, by comparing the results in Table II with Fig. 7, one can find

(3)

TABLE I  
AVAILABLE MACROCELL CHANNEL SETS FOR THE 100 MICROAREAS IN FIG. 5

zone	channel set	zone	channel set	zone	channel set	zone	channel set
1	$7_\alpha, 7_\beta$	26	$6_\alpha, 6_\gamma$	51	$6_\alpha, 6_\beta$	76	$3_\alpha, 3_\beta$
2	$5_\beta, 5_\gamma$	27	$7_\alpha, 7_\gamma$	52	$7_\alpha, 7_\beta$	77	$6_\alpha, 6_\gamma$
3	$1_\beta, 1_\gamma$	28	$5_\alpha, 5_\beta$	53	$5_\beta, 5_\gamma$	78	$7_\alpha, 7_\gamma$
4	$2_\beta, 2_\gamma$	29	$1_\alpha, 1_\beta$	54	$1_\beta, 1_\gamma$	79	$5_\alpha, 5_\beta$
5	$4_\alpha, 4_\gamma$	30	$2_\alpha, 2_\beta$	55	$2_\beta, 2_\gamma$	80	$1_\alpha, 1_\beta$
6	$3_\alpha, 3_\gamma$	31	$3_\alpha, 3_\beta$	56	$4_\alpha, 4_\gamma$	81	$4_\alpha, 4_\beta$
7	$6_\beta, 6_\gamma$	32	$6_\alpha, 6_\gamma$	57	$3_\alpha, 3_\gamma$	82	$3_\alpha, 3_\beta$
8	$7_\beta, 7_\gamma$	33	$7_\alpha, 7_\gamma$	58	$6_\beta, 6_\gamma$	83	$6_\alpha, 6_\gamma$
9	$5_\alpha, 5_\gamma$	34	$5_\alpha, 5_\beta$	59	$7_\beta, 7_\gamma$	84	$7_\alpha, 7_\gamma$
10	$1_\alpha, 1_\gamma$	35	$1_\alpha, 1_\beta$	60	$5_\alpha, 5_\gamma$	85	$5_\alpha, 5_\beta$
11	$4_\alpha, 4_\gamma$	36	$2_\alpha, 2_\beta$	61	$2_\beta, 2_\gamma$	86	$1_\alpha, 1_\beta$
12	$3_\alpha, 3_\gamma$	37	$4_\beta, 4_\gamma$	62	$4_\alpha, 4_\gamma$	87	$2_\alpha, 2_\beta$
13	$6_\beta, 6_\gamma$	38	$3_\beta, 3_\gamma$	63	$3_\alpha, 3_\gamma$	88	$4_\beta, 4_\gamma$
14	$7_\beta, 7_\gamma$	39	$6_\alpha, 6_\beta$	64	$6_\beta, 6_\gamma$	89	$3_\beta, 3_\gamma$
15	$5_\alpha, 5_\gamma$	40	$7_\alpha, 7_\beta$	65	$7_\beta, 7_\gamma$	90	$6_\alpha, 6_\beta$
16	$1_\alpha, 1_\gamma$	41	$1_\alpha, 1_\beta$	66	$5_\alpha, 5_\gamma$	91	$5_\alpha, 5_\beta$
17	$2_\alpha, 2_\gamma$	42	$2_\alpha, 2_\beta$	67	$1_\alpha, 1_\gamma$	92	$1_\alpha, 1_\beta$
18	$4_\alpha, 4_\beta$	43	$4_\beta, 4_\gamma$	68	$2_\alpha, 2_\gamma$	93	$2_\alpha, 2_\beta$
19	$3_\alpha, 3_\beta$	44	$3_\beta, 3_\gamma$	69	$4_\alpha, 4_\beta$	94	$4_\beta, 4_\gamma$
20	$6_\alpha, 6_\gamma$	45	$6_\alpha, 6_\beta$	70	$3_\alpha, 3_\beta$	95	$3_\beta, 3_\gamma$
21	$5_\alpha, 5_\gamma$	46	$7_\alpha, 7_\beta$	71	$7_\beta, 7_\gamma$	96	$6_\alpha, 6_\beta$
22	$1_\alpha, 1_\gamma$	47	$5_\beta, 5_\gamma$	72	$5_\alpha, 5_\beta$	97	$7_\alpha, 7_\beta$
23	$2_\alpha, 2_\gamma$	48	$1_\beta, 1_\gamma$	73	$1_\alpha, 1_\gamma$	98	$5_\beta, 5_\gamma$
24	$4_\alpha, 4_\beta$	49	$2_\beta, 2_\gamma$	74	$2_\alpha, 2_\gamma$	99	$1_\beta, 1_\gamma$
25	$3_\alpha, 3_\beta$	50	$4_\alpha, 4_\gamma$	75	$4_\alpha, 4_\beta$	100	$2_\beta, 2_\gamma$

that the second-tier interfering BS's only degrade the S/I by about 0.5 dB.

### B. Uplink Cochannel Interference Analysis

By modifying (2) slightly, we can formulate the uplink S/I performance as

$$\frac{S_M^u}{I_M^u + J_{\mu M}^u} = \frac{p_{t,m}^M \frac{(h_b^M h_m)^2}{R_M^A}}{\sum_{i=1}^{N_M} \frac{p_{t,m}^M (h_b^M h_m)^2}{D_i^A} + \sum_{j=1}^{Z_\mu} \sum_{k=1}^{C_\mu} \frac{p_{t,m}^\mu (h_b^M h_m)^2}{d_{jk}^A}} \quad (4)$$

where

- $S_M^u$  macrocell BS received power from the desired MS;
- $I_M^u$  uplink macrocell-to-macrocell interference;
- $J_{\mu M}^u$  uplink microcell-to-macrocell interference;
- $P_{t,m}^M$  macrocell MS transmitted power;
- $P_{t,m}^\mu$  microcell MS transmitted power.

The other parameters are defined following (2). With directional antennas, the macrocell BS's experience fewer interfering microareas in the uplink direction as compared with the downlink direction. Consider the macrocell sector that is assigned with channel set  $2_\gamma$  and near microarea 37. This macrocell sector encounters two first-tier MS's and four second-tier macrocell interfering MS's with  $[D_1, D_2, D_3, D_4, D_5, D_6] = [3.61, 3.61, 8.54, 8.19, 8.19, 7.81]R_M$  and interfering microareas 23, 55, 61, 68, 74, and 100 (i.e.,  $Z_\mu = 6$ ) with  $[d_1, d_2, d_3, d_4, d_5, d_6] = [7.0, 7.0, 14.7, 5.3, 11.5, 9.53]R_M$ .

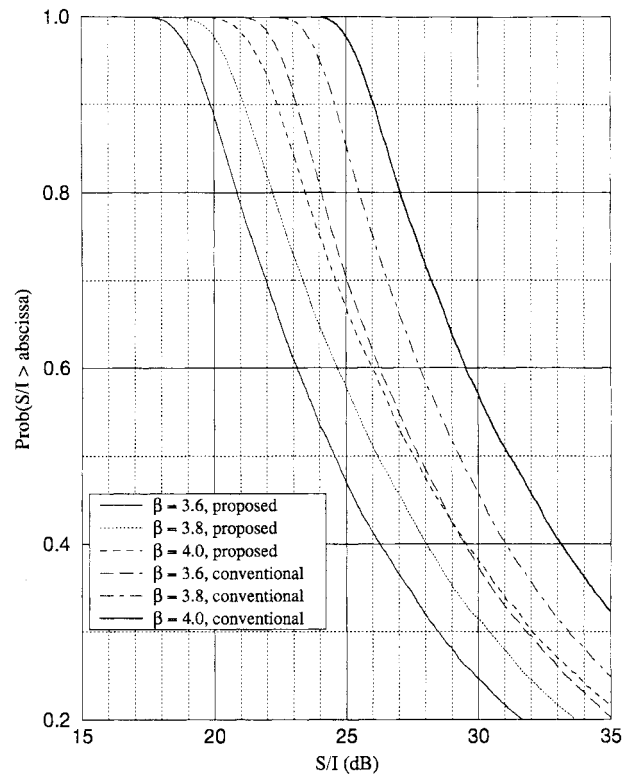


Fig. 6. Comparison of the uplink S/I performance of conventional macrocells and the proposed hierarchical cellular system without underlaid microcells for different path-loss exponent  $\beta$ .

We ignore the effect of the three other interfering microareas 4, 17, and 49 because they are located in the back-lobe area

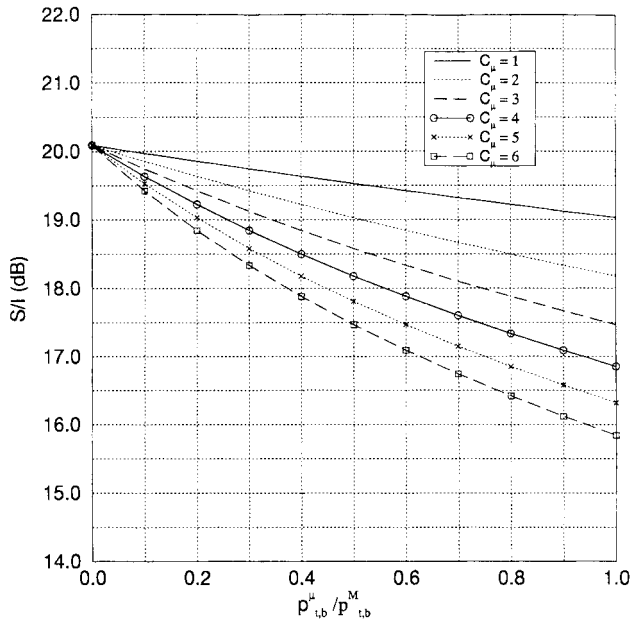


Fig. 7. Macrocell downlink S/I performance against  $p_{t,b}^{\mu}/p_{t,b}^M$  for different values of  $C_{\mu}$ , where  $p_{t,b}^{\mu}/p_{t,b}^M$  is the ratio of the transmitted power of the microcell BS to that of the macrocell BS and  $C_{\mu}$  is the number of microcell clusters in a microarea.

of the sector using channel set  $2\gamma$ . By substituting the above values into (4), the uplink S/I performance for this example becomes

$$\frac{S_M^u}{I_M^u + J_{\mu M}^u} = \frac{1}{1.2677 \times 10^{-2} + C_{\mu} \left( \frac{p_{t,m}^{\mu}}{p_{t,m}^M} \right) \times 2.11 \times 10^{-3}}. \quad (5)$$

Fig. 8 shows the results. It is observed that S/I is higher than 18 dB for  $C_{\mu} = 1 \sim 6$  if

$$\frac{p_{t,m}^{\mu}}{p_{t,m}^M} \leq 0.2. \quad (6)$$

Note that we obtained (6) by assuming that the interfering macrocell MS's are on the cell boundary and are transmitting with the maximum power. Thus, (6) can be used to determine the maximum microcell MS's transmitted power. For the IS-54 Class-IV portable handset (that adjusts its transmitted power in six levels from  $-22$  to  $-2$  dBW), (6) implies that the maximum microcell MS transmitted power is  $-9$  dBW, which is still in the operation range of the Class-IV terminal. Thus, the requirement in (6) can be fulfilled by the current uplink power control scheme in IS-54 system without changing the MS transmitted-power specification.

## VI. MICROCELL PERFORMANCE

This section studies how to determine the microcell size to achieve the required S/I performance.

TABLE II  
DOWNLINK S/I PERFORMANCE FOR OVERLAYING  
MACROCELLS, WHERE  $h_b^{\mu}/h_b^M = 1/3$

$\frac{p_{t,b}^{\mu}}{p_{t,b}^M}$	$S_M^d/(I_M^d + J_{\mu M}^d)$ (dB)			
	$C_{\mu} = 1$	$C_{\mu} = 2$	$C_{\mu} = 4$	$C_{\mu} = 6$
0	19.88	19.88	19.88	19.84
0.1	19.76	19.64	19.42	18.22
0.2	19.65	19.42	19.02	18.65
0.3	19.53	19.22	18.65	18.15
0.4	19.43	19.02	18.31	17.70
0.5	19.32	18.83	17.99	17.29
0.6	19.22	18.65	17.69	16.91
0.7	19.12	18.48	17.42	16.57
0.8	19.02	18.30	17.16	16.25
0.9	18.93	18.14	16.91	15.96
1.0	18.83	17.99	16.68	15.68

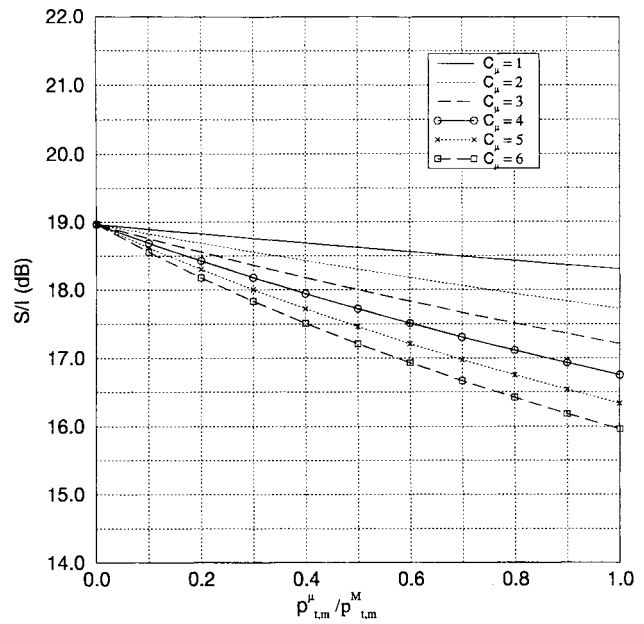


Fig. 8. Macrocell uplink S/I performance against  $p_{t,m}^{\mu}/p_{t,m}^M$  for different values of  $C_{\mu}$ , where  $p_{t,m}^{\mu}/p_{t,m}^M$  is the ratio of the transmitted power of the microcell MS to that of the macrocell MS and  $C_{\mu}$  is the number of microcell clusters in a microarea.

### A. Downlink Microcell Size

A feasible microcell size should satisfy two conditions: 1) *S-criterion*: an MS will receive stronger power  $S$  at the microcell boundary than at the macrocell boundary and 2) *S/I-criterion*: the signal-to-interference ratio (S/I) at the microcell boundary is equal to or better than that at the macrocell boundary.

1) *S-criterion*: From the path-loss model in (1), the microcell radius  $R_{\mu}$  can be calculated as

$$R_{\mu} \leq \left[ \left( \frac{p_{t,b}^{\mu}}{p_{t,b}^M} \right) \left( \frac{h_b^{\mu}}{h_b^M} \right)^2 \right]^{1/4} R_M \quad (7)$$

where  $R_M$ ,  $h_b^{\mu}$ ,  $h_b^M$ ,  $p_{t,b}^{\mu}$ , and  $p_{t,b}^M$  are defined in (2).

2) *S/I-criterion*: The S/I received by the MS at the microcell boundary can be written as (8), given at the bottom of the



page, where the parameters  $p_{t,b}^\mu$ ,  $p_{t,b}^M$ ,  $h_b^M$ ,  $h_b^\mu$ ,  $C_\mu$ , and  $h_m$  are already defined in (2) and

$S_\mu^d$	MS received power from its desired microcell BS;
$I_\mu^d$	downlink microcell-to-microcell interference;
$J_{M\mu}^d$	downlink macrocell-to-microcell interference;
$N_{Mf}$	number of main-lobe macrocell interferers;
$N_{Mb}$	number of back-lobe macrocell interferers;
$D_{Mf,i}$	MS distance to the $i$ th main-lobe interfering BS;
$D_{Mb,j}$	MS distance to the $j$ th back-lobe interfering BS;
$D_{\mu i}$	MS distance to the $i$ th microcell interfering BS;
$R_M$	macrocell radius;
$R_\mu$	microcell radius;
$\eta$	front-to-back ratio of the directional antenna in macrocells.

Let  $(S/I)_{\text{req}}$  denote the required S/I. Then, (8) becomes (9), given at the bottom of the page, where

$$\widehat{D}_{Mf,i} = D_{Mf,i}/R_M, \quad \widehat{D}_{Mb,j} = D_{Mb,j}/R_M, \quad \text{and} \\ \widehat{D}_{\mu i} = D_{\mu i}/R_M$$

are the normalized distances of interferers with respect to macrocell radius  $R_M$ . Our studies assume that the microcells and macrocells have similar shapes and that the microcell clusters are adjacent to each other in a given microarea. Suppose the distances from a microcell MS to its interfering microcell BS's are equal and close to the microcell cochannel reuse distance  $D_\mu$  (i.e.,  $D_{\mu,i} = D_\mu$ , for  $i = 1, \dots, C_\mu$ ). Then, we have [7]

$$D_\mu = \sqrt{3K_\mu}R_\mu \quad (10)$$

where  $K_\mu$  denotes the microcell cluster size. With  $C_\mu$  microcell clusters and  $K_\mu$  microcells inside each cluster, a microarea has in total  $C_\mu K_\mu$  microcells. Suppose that taken together they are smaller than the area of a macrocell. Then

$$R_M \geq \sqrt{C_\mu K_\mu}R_\mu, \quad (11)$$

Substituting (10) and (11) into (9), we get (12), given at the bottom of the next page. Notice that we consider  $N_{Mb}$  back-lobe macrocell interferers in (12). The back-lobe interference from the macrocell BS's can be ignored for the macrocell

MS, but for the microcell MS this kind of interference may be relatively strong compared to the received signal strength from the *low-powered* microcell BS. For the same reason, the macrocell interferers in the second ring are considered here.

a) *Example:* Referring to Fig. 5 and Table I, microarea 56 can be assigned channel sets  $[4_\alpha, 4_\gamma]$ . Take channel set  $4_\gamma$  as an example. Microarea 56 will experience three first-tier back-lobe interferers ( $N_{Mb} = 3$ ), each of which has the following distance:

$$[\widehat{D}_{Mb,1}, \widehat{D}_{Mb,2}, \widehat{D}_{Mb,3}] = [2.65, 2.65, 2.65] \quad (13)$$

to the center of microarea 56. Three main-lobe interfering macrocells in the second tier are located near microareas 25, 79, and 64 with the distances of

$$[\widehat{D}_{Mf,1}, \widehat{D}_{Mf,2}, \widehat{D}_{Mf,3}] = [5.29, 5.29, 5.29]. \quad (14)$$

Additionally, three main-lobe interfering macrocell BS's in the third tier are located near microareas 13, 70, and 85 with distances of

$$[\widehat{D}_{Mf,4}, \widehat{D}_{Mf,5}, \widehat{D}_{Mf,6}] = [7.0, 7.0, 7.0]. \quad (15)$$

It is also important to determine if there exists interfering microcell BS's from neighboring microareas. From Fig. 5 and Table I, one can find one feature of the proposed system architecture—the adjacent microareas are assigned with different macrocell channel sets. For instance, microarea 56 in Fig. 5 is assigned with the channel sets  $[4_\alpha, 4_\gamma]$ . The neighboring microareas 45, 46, 55, 57, 66, and 67 use channel sets  $[6_\alpha, 6_\beta]$ ,  $[7_\alpha, 7_\beta]$ ,  $[2_\beta, 2_\gamma]$ ,  $[3_\alpha, 3_\gamma]$ ,  $[5_\alpha, 5_\gamma]$ , and  $[1_\alpha, 1_\gamma]$ . It is obvious that when considering the interfering microcell BS's, a microcell MS will only be affected by the interfering microcell BS's in the same microarea. Assume that each microarea consists of  $C_\mu$  microcell clusters. Then, an MS will experience the interference from the remaining  $C_\mu - 1$  microcell BS's, excluding the desired one. Substituting (13), (14), and (15) into (12), one can obtain (16), given at the bottom of the next page.

$$\frac{S_\mu^d}{I_\mu^d + J_{M\mu}^d} = \frac{p_{t,b}^\mu \frac{(h_{\mu,b}h_m)^2}{R_\mu^4}}{\sum_{i=1}^{C_\mu-1} \frac{p_{t,b}^\mu (h_{\mu,b}h_m)^2}{D_{\mu i}^4} + \sum_{i=1}^{N_{Mf}} \frac{p_{t,b}^M (h_{M,b}h_m)^2}{D_{Mf,i}^4} + \frac{1}{\eta} \left( \sum_{i=1}^{N_{Mb}} \frac{p_{t,b}^M (h_{M,b}h_m)^2}{D_{Mb,i}^4} \right)}. \quad (8)$$

$$\frac{R_\mu}{R_M} \leq \left[ \frac{(S/I)_{\text{req}}^{-1}}{\sum_{i=1}^{C_\mu-1} \left( \frac{1}{\widehat{D}_{\mu i}} \right)^4 + \left( \sum_{i=1}^{N_{Mf}} \left( \frac{1}{\widehat{D}_{Mf,i}} \right)^4 + \frac{1}{\eta} \sum_{j=1}^{N_{Mb}} \left( \frac{1}{\widehat{D}_{Mb,j}} \right)^4 \right) \left( \frac{p_{t,b}^M}{p_{t,b}^\mu} \right) \left( \frac{h_{M,b}}{h_{\mu,b}} \right)^2} \right]^{1/4}. \quad (9)$$

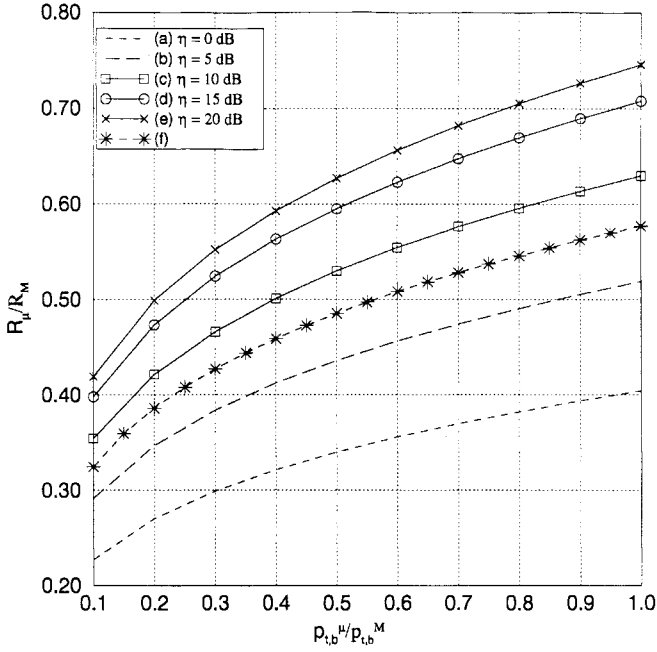


Fig. 9. Effect of front-to-back ratio  $\eta$  on the microcell radius based on downlink microcell S/I performance analysis, where  $R_\mu/R_M$  and  $p_{t,b}^\mu/p_{t,b}^M$  are the cell radius ratio and transmitted-power ratio of microcells over macrocells, respectively. With  $(S/I)_{\text{req}} = 18$  dB and  $h_b^\mu/h_b^M = 1/3$ , curves (a) ~ (e) are obtained by S/I-criterion for  $\eta = 0, 5, 10, 15$ , and 20 dB, respectively, while curve (f) is obtained by S-criterion.

- 1)  $C_\mu = 1$ : We first consider a special case, where only one microcell is installed in a microarea. In the beginning stage, this may occur when a large underlaid microcell is first installed to release traffic load of the macrocellular system. Fig. 9 shows the effect of the front-to-back ratio  $\eta$  on the microcell radius, whereby  $(S/I)_{\text{req}} = 18$  dB and  $h_b^\mu/h_b^M = 1/3$ . If the S/I- and S-criterion result in different microcell radii, then the smaller one will be chosen. From Fig. 9, one can observe that if front-to-back ratio  $\eta \geq 10$  dB, the microcell radius is determined by the S-criterion, but when  $\eta \leq 5$  dB, the S/I-criterion

dominates the S-criterion. For instance, in the case of  $\eta = 10$  dB and  $p_{t,b}^\mu/p_{t,b}^M = 0.4$ , one can obtain  $R_\mu \leq 0.5R_M$  by the S/I-criterion and  $R_\mu \leq 0.46R_M$  by the S-criterion, respectively. For choosing the smaller one, the microcell radius is therefore  $0.46R_M$ . In this example, one can see that a larger front-to-back ratio  $\eta$  does not imply a larger microcell size since the S-criterion, which is independent of  $\eta$ , will dominate the S/I-criterion when  $\eta$  is large.

- 2)  $C_\mu \geq 2$ : Next, we consider the case when many microcells are deployed in each microarea. Fig. 10 shows the downlink microcell size against  $p_{t,b}^\mu/p_{t,b}^M$  for different values of  $C_\mu$ , where  $p_{t,b}^\mu/p_{t,b}^M$  is the ratio of the transmitted power of the microcell BS to that of the macrocell BS and  $C_\mu$  is the number of microcell clusters in a microarea. It is observed that if  $C_\mu \geq 3$ ,  $p_{t,b}^\mu/p_{t,b}^M$  has little effect on the downlink microcell size. This is because the interference from the microcells  $I_\mu^d$  will dominate the macrocell interference  $J_\mu^d$  when the number of cochannel microcells  $(C_\mu - 1)$  becomes large in a given microarea. In other words, if a large number of microcells are installed, the S/I-criterion will become a dominating factor in determining the microcell size. In the case  $C_\mu = 6$ , for example, one should follow the S/I-criterion to get  $R_\mu \leq 0.165R_M$  from Fig. 10.

### B. Uplink Microcell Size

Similar to the former analysis, the uplink microcell size is derived from the S/I analysis. More specifically

$$\begin{aligned} \frac{S_\mu^u}{I_\mu^u + J_{M\mu}^u} &= \frac{p_{t,m}^\mu \frac{(h_b^\mu h_m)^2}{R_{\mu,up}^4}}{\sum_{i=1}^{C_\mu-1} \frac{p_{t,m}^\mu (h_b^\mu h_m)^2}{D_{\mu_i}^4} + \sum_{i=1}^{N_{Mf}} \frac{p_{t,m}^M (h_b^M h_m)^2}{D_{M_i}^4}} \quad (17) \end{aligned}$$

$$\frac{R_\mu}{R_M} \leq \left[ \frac{(S/I)_{\text{req}}^{-1}}{\frac{(C_\mu - 1)C_\mu^2}{9} + \left( \sum_{i=1}^{N_{Mf}} \left( \frac{1}{D_{Mf,i}} \right)^4 + \frac{1}{\eta} \sum_{j=1}^{N_{Mb}} \left( \frac{1}{D_{Mb,j}} \right)^4 \right) \left( \frac{p_{t,b}^M}{p_{t,b}^\mu} \right) \left( \frac{h_b^M}{h_b^\mu} \right)^2} \right]^{1/4} \quad (12)$$

$$\frac{R_\mu}{R_M} \leq \left[ \frac{(S/I)_{\text{req}}^{-1}}{\frac{(C_\mu - 1)C_\mu^2}{9} + \left( 5.0803 \times 10^{-3} + 0.0608 \times \frac{1}{\eta} \right) \left( \frac{p_{t,b}^M}{p_{t,b}^\mu} \right) \left( \frac{h_b^M}{h_b^\mu} \right)^2} \right]^{1/4} \quad (16)$$

where the parameters  $p_{t,b}^\mu$ ,  $p_{t,b}^M$ ,  $C_\mu h_b^M$ ,  $D_{\mu,i}$ ,  $R_M$ ,  $h_b^\mu$ , and  $h_m$  have been defined in (2) and (8) and

- $S_\mu^u$  microcell BS received power from the desired microcell MS;
- $I_{\mu M}^u$  uplink microcell-to-macrocell interference;
- $J_{M\mu}^u$  uplink macrocell-to-microcell interference;
- $N_{M,f}$  number of macrocell interfering MS's;
- $D_{M,i}$  BS distance to the  $i$ th interfering macrocell MS;
- $R_{\mu,up}$  uplink microcell radius.

Let  $D_{M,i} = \widehat{D}_{M,i} R_M$  and  $(S/I)_{req}$  denote the required S/I for a microcell BS. Using the same assumptions for getting (12), one can simplify (17) as

$$\frac{R_{\mu,up}}{R_M} \leq \left[ \frac{(S/I)_{req}^{-1}}{\frac{(C_\mu - 1)C_\mu^2}{9} + \left( \sum_{i=1}^{N_{M,f}} \left( \frac{1}{\widehat{D}_{M,f,i}} \right)^4 \right) \left( \frac{p_{t,m}^M}{p_{t,m}^\mu} \right)} \right]^{1/4}. \quad (18)$$

In Section VI-A, we have shown that when the number of microcell clusters  $C_\mu$  becomes large, the downlink microcell size is insensitive to the interference from the macrocell. This is also true for determining the uplink microcell size. This will be shown by an example later. When microcell interference dominates the performance, (18) can be approximated as

$$\frac{R_{\mu,up}}{R_M} \leq \left[ \frac{1}{(S/I)_{req} \frac{(C_\mu - 1)C_\mu^2}{9}} \right]^{1/4}. \quad (19)$$

By combining (10), (11), and (19), we obtain the upper and lower bounds of  $K_\mu$  as

$$\frac{1}{3} \sqrt{(S/I)_{req} (C_\mu - 1)} \leq K_\mu \leq \frac{1}{C_\mu} \left( \frac{R_M}{R_\mu} \right)^2. \quad (20)$$

The relation between  $K_\mu$  and  $C_\mu$  with  $R_\mu/R_M$  as a parameter is shown in Fig. 11.

1) *Example:* Consider again microarea 56 in Fig. 5. Referring to Table I, microarea 56 can be assigned channel sets  $[4_\alpha, 4_\gamma]$ . Take channel set  $4_\alpha$ , for example. The worst case occurs when interfering macrocell MS's transmit maximum power, i.e., at the macrocell boundary. For the example considered, the three first-tier interfering macrocell MS's near microareas 45, 47, and 77 are at distances  $[\widehat{D}_{M,1}, \widehat{D}_{M,2}, \widehat{D}_{M,3}] = [2.0, 2.0, 2.0]$ ; the three second-tier interfering macrocell MS's near microareas 26, 53, and 89 are at distances  $[\widehat{D}_{M,4}, \widehat{D}_{M,5}, \widehat{D}_{M,6}] = [4.36, 4.36, 4.36]$ ; the three third-tier interfering macrocell MS's near microareas 32, 38, and 98 are at distances  $[\widehat{D}_{M,7}, \widehat{D}_{M,8}, \widehat{D}_{M,9}] = [6.0, 6.0, 6.0]$ . Substituting these values into (18) and letting  $(S/I)_{req} = 18$  dB, we show in Fig. 12 the ratio of microcell radius to macrocell radius  $R_\mu/R_M$  against  $p_{t,m}^\mu/p_{t,m}^M$  for different values of  $C_\mu$ , where  $p_{t,m}^\mu/p_{t,m}^M$  is the ratio of the transmitted power of the microcell MS to that of the macrocell MS and  $C_\mu$  is the number of the microcell clusters in a

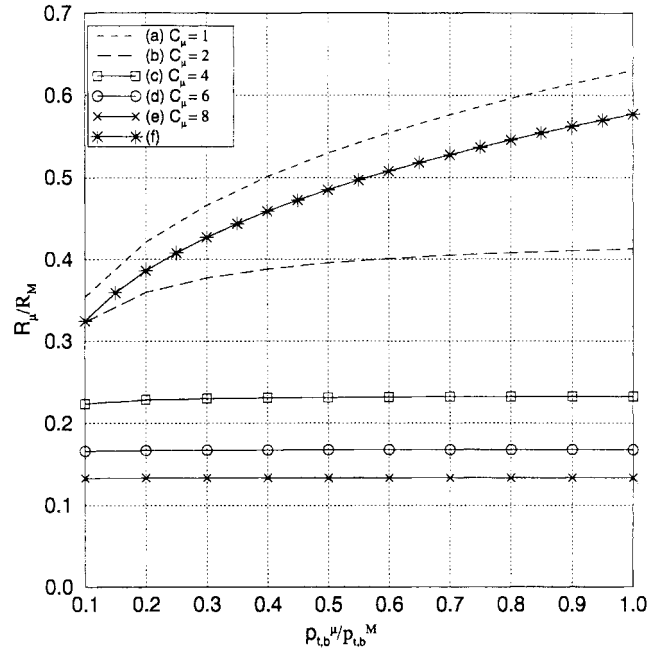


Fig. 10. Downlink microcell radius  $R_\mu$  against  $p_{t,b}^\mu/p_{t,b}^M$  for different values of  $C_\mu$  in the case  $\eta = 10$  dB,  $(S/I)_{req} = 18$  dB, and  $h_b^\mu/h_b^M = 1/3$ , whereby the microcell radius is normalized with respect to the macrocell radius  $R_M$ ;  $p_{t,b}^\mu/p_{t,b}^M$  represents the ratio of the transmitted power of microcell BS to that of macrocell BS; and  $C_\mu$  is the number of clusters in a microarea;  $\eta$  is the front-to-back ratio of the directional antenna;  $h_b^\mu/h_b^M$  is the ratio of the microcell BS antenna to the macrocell BS antenna. Curves (a) ~ (e) are obtained by S/I-criterion for  $C_\mu = 1, 2, 4, 6$ , and  $8$ , while curve (f) is obtained by S-criterion.

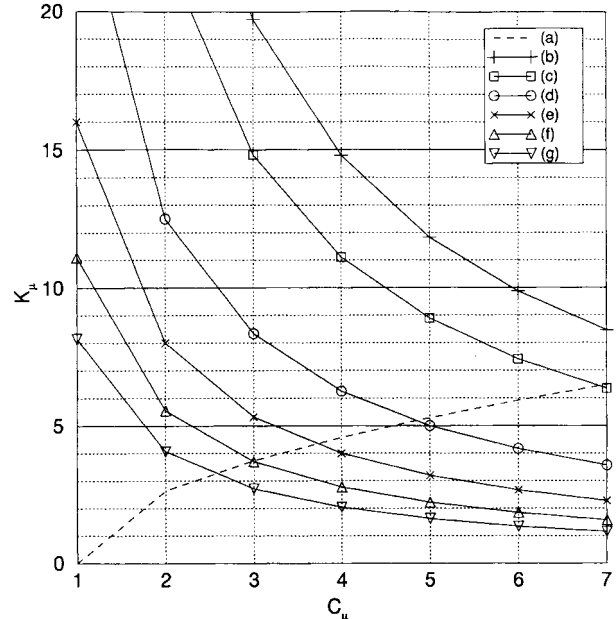


Fig. 11.  $K_\mu$  against  $C_\mu$  with  $R_\mu/R_M$  as a parameter, whereby  $K_\mu$  is the microcell cluster size,  $C_\mu$  is the number of clusters in a microarea, and  $R_\mu/R_M$  is the ratio of the microcell radius to the macrocell radius. Curve (a) represents the lower bound of  $K_\mu$ , while curves (b) ~ (g) represent the upper bound of  $K_\mu$  for  $R_\mu/R_M = 0.13, 0.15, 0.20, 0.25, 0.30$ , and  $0.35$ , respectively.

microarea. It is shown that as  $C_\mu$  increases, microcell size becomes insensitive to  $p_{t,m}^\mu/p_{t,m}^M$ . Suppose our objective is

TABLE III  
FREQUENCY MANAGEMENT PLAN FOR AVOIDING ADJACENT CHANNEL INTERFERENCE

1 $\alpha$	1	22	43	64	85	106	127	148	169	190	211	232	253	274	295	316
2 $\alpha$	2	23	44	65	86	107	128	149	170	191	212	233	254	275	296	317
3 $\alpha$	3	24	45	66	87	108	129	150	171	192	213	234	255	276	297	318
4 $\alpha$	4	25	46	67	88	109	130	151	172	193	214	235	256	277	298	319
5 $\alpha$	5	26	47	68	89	110	131	152	173	194	215	236	257	278	299	320
6 $\alpha$	6	27	48	69	90	111	132	153	174	195	216	237	258	279	300	321
7 $\alpha$	7	28	49	70	91	112	133	154	175	196	217	238	259	280	301	322
1 $\beta$	8	29	50	71	92	113	134	155	176	197	218	239	260	281	302	323
2 $\beta$	9	30	51	72	93	114	135	156	177	198	219	249	261	282	303	324
3 $\beta$	10	31	52	73	94	115	136	157	178	199	220	250	262	283	304	325
4 $\beta$	11	32	53	74	95	116	137	158	179	200	221	251	263	284	305	326
5 $\beta$	12	33	54	75	96	117	138	159	180	201	222	252	264	285	306	327
6 $\beta$	13	34	55	76	97	118	139	160	181	202	223	253	265	286	307	328
7 $\beta$	14	35	56	77	98	119	140	161	182	203	224	254	266	287	308	329
1 $\gamma$	15	36	57	78	99	120	141	162	183	204	225	255	267	288	309	330
2 $\gamma$	16	37	58	79	100	121	142	163	184	205	226	256	268	289	310	331
3 $\gamma$	17	38	59	80	101	122	143	164	185	206	227	257	269	290	311	332
4 $\gamma$	18	39	60	81	102	123	144	165	186	207	228	258	270	291	312	333
5 $\gamma$	19	40	61	82	103	124	145	166	187	208	221	251	271	292	313	
6 $\gamma$	20	41	62	83	104	125	146	167	188	209	222	252	272	293	314	
7 $\gamma$	21	42	63	84	105	126	147	168	189	210	223	253	273	294	315	

to implement six microcell clusters in each macroarea (i.e.,  $C_\mu = 6$ ) and still maintain  $(S/I)_{\text{req}} = 18$  dB. We first need to know the feasible cluster size  $K_\mu$  and the microcell radius. From Fig. 11, we obtain  $K_\mu = 7$  and  $R_\mu = 0.15 \times R_M$ . Then, from Fig. 12, we find the transmitted power for a microcell MS should be at least 0.017 times that for a macrocell MS. Consider an interfering macrocell MS, which is an IS-54 Class-IV portable handset transmitting at  $-2$  dBW. Thus, the microcell MS transmitted power should be larger than  $-20$  dBW in this case. Recall the transmitted power of an IS-54 Class-IV portable handset ranges from  $-22$  to  $-2$  dBW. Consequently, the current IS-54 Class-IV portable handset can be used in both the macrocells and microcells of the proposed system architecture without changing the handset transmit power specification.

## VII. ADJACENT CHANNEL INTERFERENCE ANALYSIS

In this section, we review a frequency management plan to avoid adjacent channel interference in the conventional macrocellular system. Then, we examine if this management scheme still works for the proposed hierarchical cellular system. As shown in Fig. 1, a traditional seven-cell macrocellular system has 21 sectors. If 10 MHz of spectrum is used and each channel occupies 30 KHz, then a total of 333 carriers will be assigned to the 21 sectors. A frequency plan to avoid adjacent channel interference is shown in Table III [7]. Each row in the table represents a frequency set that is designated to a sector. This scheme separates any two carriers assigned to adjacent sectors by seven carriers.

Applying the frequency plan in Table III to the proposed hierarchical cellular system (Fig. 5), we can easily see that there is no adjacent channel interference between macrocell sectors. Even with the addition of underlaid microcells,

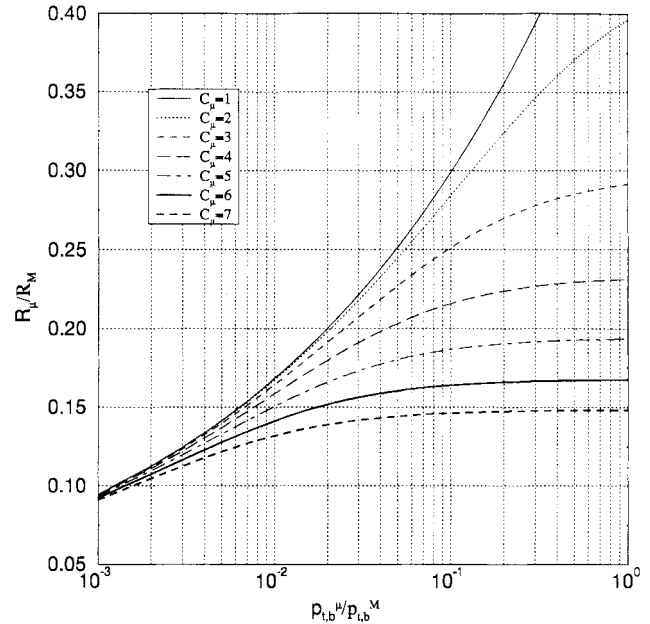


Fig. 12. Uplink microcell radius  $R_\mu$  against  $p_{t,m}^\mu/p_{t,m}^M$  for different values of  $C_\mu$ , where the microcell radius is normalized by the macrocell radius  $R_M$ ,  $p_{t,m}^\mu/p_{t,m}^M$  is the ratio of the transmitted power of the microcell MS to that of the macrocell MS,  $C_\mu$  is the number of microcell clusters in a macroarea, and  $(S/I)_{\text{req}} = 18$  dB.

a two-carrier separation is maintained for the carriers assigned to the microcells and the cosite macrocells within a macroarea. For example, referring to Fig. 5 and Table I, the channel set  $[4\alpha, 4\gamma]$  is assigned to macroarea 56. The cosite macrocell sectors that use channel set  $1\beta$ ,  $2\alpha$ , and  $7\gamma$  have at least a two-carrier separation. This feature is valid for all the macroareas with channel assignment of Table I.

### VIII. CONCLUDING REMARKS

This paper has proposed a new sectoring scheme, which allows underlaid microcells to reuse macrocell frequencies. For each area consisting of three macrocell sectors, the proposed architecture can reuse another *two* macrocell channel sets *six* times while retaining  $S/I \geq 18$  dB. Hence, the system capacity of the proposed architecture can be five times that of a traditional three-sector  $N = 7$  cellular system (Fig. 1). If the  $S/I$  requirement can be lowered, e.g., 9 dB in the global system for mobile communications (GSM), then the improvement can be even larger. The capacity improvement of the proposed architecture is achieved by deploying a large number of underlaid microcells. This feature, however, cannot be easily done in other sectorized cellular architectures, e.g., those in [8] and [9]. The proposed architecture allows microcells to be deployed throughout the entire area, and allows them to be gradually introduced to match the increasing demand of the cellular service. With these flexibilities, the proposed architecture allows the existing macrocellular systems to smoothly evolve into hierarchical microcell/macrocell systems.

### REFERENCES

- [1] L.-R. Hu and S. S. Rappaport, "Personal communication systems using multiple hierarchical cellular overlays," *IEEE J. Select. Areas Commun.*, vol. 13, pp. 406–415, Feb. 1995.
- [2] C. W. Sung and W. S. Wong, "User speed estimation and dynamic channel allocation in hierarchical cellular system," in *IEEE Veh. Technol. Conf.*, 1994, pp. 91–95.
- [3] C. L. I, L. J. Greenstein, and R. Gitlin, "A microcell/macrocell cellular architecture for low- and high-mobility wireless users," *IEEE J. Select. Areas Commun.*, vol. 11, pp. 885–891, 1993.
- [4] T.-S. P. Yum and W.-S. Wong, "Hot-spot traffic relief in cellular systems," *IEEE J. Select. Areas Commun.*, vol. 11, pp. 934–940, 1993.
- [5] H. Furukawa and Y. Akiwa, "A microcell overlaid with umbrella cell system," in *IEEE Veh. Technol. Conf.*, 1994, pp. 1455–1459.
- [6] EIA/TIA/IS-54-A, *Cellular System Dual-Mode Mobile Station—Base Station Compatibility Standard*, 1991.
- [7] W. C. Y. Lee, *Mobile Communications Design Fundamentals*. New York: Wiley, 1993.
- [8] ———, "Smaller cells for greater performance," *IEEE Commun. Mag.*, pp. 19–23, Nov. 1991.
- [9] G. K. Chan, "Effects of sectorization on the spectrum efficiency of cellular radio systems," *IEEE Trans. Veh. Technol.*, vol. 41, pp. 217–225, 1992.



**Li-Chun Wang** (S'93–M'96) received the B.S. degree from National Chiao Tung University, Hsinchu, Taiwan, R.O.C., in 1986, the M.S. degree from National Taiwan University, Taipei, Taiwan, in 1988, and the Ph.D. degree from the Georgia Institute of Technology, Atlanta, in 1996, all in electrical engineering.

From 1990 to 1992, he was with Telecommunication Laboratories, Taiwan, where he worked on wireless PBX. From 1992 and 1996, he was a Doctoral Candidate researching channel modeling and architectures for cellular-based personal communications. During his Ph.D. study in 1995, he worked for Nortel in Richardson, TX. Since July 1996, he has been with the Wireless Communications Research Department of AT&T Labs, Red Bank, NJ. His current research interests are in cellular architectures and radio resource management for personal communications. Specific topics include interference analysis, macrodiversity systems, and hierarchical cellular architectures.

**Gordon L. Stüber** (S'81–M'86–SM'96) received the B.A.Sc. and Ph.D. degrees in electrical engineering from the University of Waterloo, Waterloo, Ont., Canada, in 1982 and 1986, respectively.

In 1986, he joined the School of Electrical Engineering, Georgia Institute of Technology, Atlanta, where he is currently a Professor. His research interests are in wireless communications and communication signal processing, with emphasis on radio link and receiver design and radio resource management. He is the author of the textbook *Principles of Mobile Communication* (Norwell, MA: Kluwer, 1996).

Dr. Stüber is an active Member of the IEEE Communication and Vehicular Technology Societies. He is a Member of the COMSOC Communication Theory Committee and Technical Program Committee for ICC'94, PIMRC'95, PIMRC'96, VTC'97, and VTC'98. He served as Technical Program Chair for VTC'96 and is currently serving as Technical Program Chair for ICC'98. Since January 1993, he has been an Editor for spread spectrum with the IEEE TRANSACTIONS ON COMMUNICATIONS.

**Chin-Tau Lea** (M'82–SM'92) received the B.S. and M.S. degrees from National Taiwan University, Taiwan, R.O.C., in 1976 and 1978 and the Ph.D. degree from the University of Washington, Seattle, in 1982, all in electrical engineering.

He was with AT&T Bell Labs from 1982 to 1985. Since September 1985, he has been with the Georgia Institute of Technology, Atlanta. His current research interests are in the general area of network technologies. His recent research results include the bipartite-graph design method for solving, at the system level, the crosstalk problem of relational-type photonic switching devices. This method also led to the construction of a new class of interconnection networks for high-speed switching and parallel processing. His work on network quantization has demonstrated that quantization can be a powerful tool for solving many intractable network problems. In wireless communications, he is exploring a new network architecture of which the design principle is based on his finding that mobility and capacity are entirely convertible.